Available online at www.sciencedirect.com
SCIENCE DIRECT
Journal of Organometallic Chemistry 691 (2006) 659–666
Journal of Organometallic Chemistry
www.elsevier.com/locate/jorganchem

μ-Polymethylene bridged dicobaloximes: Structural, photolysis and thermal decomposition properties

Xin Zhang, Yizhi Li, Yuhua Mei, Huilan Chen *

Department of Chemistry, Coordination Chemistry State Key Laboratory, Nanjing University, Nanjing, Jiangsu 210093, China

Received 23 May 2005; received in revised form 4 September 2005; accepted 5 October 2005
Available online 18 November 2005

Abstract

A series of μ-polymethylene bridged dicobaloxime complexes $py(dmgH)_2Co(CH_2)_nCo(dmgH)_2$, where $n = 4$, 5, 6, and 12 (**1**–**4**) were synthesized and characterized. Crystal structures of $py(dmgH)_2Co(CH_2)_4Co(dmgH)_2py \cdot 2CH_2Cl_2$ (**1** $\cdot 2CH_2Cl_2$), $py(dmgH)_2Co(CH_2)_5Co(dmgH)_2py$ (**2**), and $py(dmgH)_2Co(CH_2)_6Co(dmgH)_2py \cdot CH_2Cl_2$ (**3** $\cdot CH_2Cl_2$) have been determined by X-ray diffraction. Their structural features are compared with those reported for monocobaloxime complexes and oligomethylene-bridged vitamin B_{12} dimer. 2-D layers or 3-D nets formed through intermolecular C–H···O interactions are observed in the molecular packing structures of **1** $\cdot 2CH_2Cl_2$, **2**, and **3** $\cdot CH_2Cl_2$. The photolytic kinetic rates of the dicobaloximes were determined by UV–Vis spectroscopy and the products of photolytic solutions were characterized by ESI-MS. The results indicated that lengths of polymethylene have a little effect on the observed rate of the Co–C bond cleavage in our dicobaloxime complexes, while changing the solvent from methanol to ethanol has shown significant rate enhancement. In addition, TGA experiments for solid dicobaloxime complexes were performed to exam their thermal decomposition behaviors.

Keywords: Organo-cobaloximes; Crystal structures; *Anti*-conformation; *Gauche*-conformation; Photolysis property; Thermal decomposition

1. Introduction

Much interest has been focused on the formation and cleavage of the metal–carbon σ-bond in organo-metallic complex, because free organic radicals would be produced during the cleavage process [1]. Especially, homolytic cleavage of the Co–C bond is generally accepted as a key step in the mechanism of action of a certain kind of enzyme, which requires a B_{12} coenzyme [2,3]. Like above enzymatic reaction, photolysis, thermolysis or electrolysis of coenzyme B_{12} and its analogues can lead to homolytic or heterolytic cleavage of the Co–C bond [4–11].

In contrast to numerous examples of organo-cobalt complexes with a single cobalt–carbon bond [9–11], there is not a plenty of work extended to organo-bridged dicobalt complexes, which are bearing two reactive Co–C bonds [12–21]. The organo-bridged dicobalt complexes are useful reagents in that they may considered to be "latent alkanediyl diradicals" [17]. Among them, μ-polymethylene bridged dicobaloxime have been paid particular interest [13,15,18], in which the metal centers are separated by an alkyl chain. They are not only as a kind of coenzyme B_{12} simulacrum [15], but also proposed as possible models for the bonding of hydrocarbon at metal surfaces [22–24]. In 1960s, Smith et al. [12] studied the preparation of dinuclear polymethylene bridged vitamin B_{12} complexes. Schrauzer [13] and Johnson [14] synthesized the first kind of μ-polymethylene bridged dicobaloxime and characterized the organic products from photolysis of these complexes by chromatography. Moss [15] systematically studied the preparation method of organobridged dicobaloximes and Gupta [18] reported *cis* influence of this kind of complexes. In 1995, the crystal structure and thermolytic properties of vitamin B_{12} dimers were reported by Kräutler [17]. Recently, spectral characterization of biphenyl- and xylylene-bridged

* Corresponding author. Tel.: +86 25 3592369.
E-mail address: hlchen@nju.edu.cn (H. Chen).

0022-328X/$ - see front matter © 2005 Elsevier B.V. All rights reserved.
doi:10.1016/j.jorganchem.2005.10.015

dicobaloximes with four different dioximes was described by Gupta et al. [21]. However, qualified single crystals for this kind of dicobaloximes have not been obtained since they are unstable in solution [21]. In this paper, we present the crystal structures analysis, photolytic and thermolysis properties of μ-polymethylene bridged dicobaloximes $py(dmgH)_2Co(CH_2)nCo(dmgH)_2py$, where $n = 4$, 5, 6, and 12 (**1**–**4**), which have varying length of alkyl chain between the two cobalt atoms. Influences of changing the alkyl chain length on the structures and crystal packing are addressed. To our knowledge, this is the first time that the X-ray structures of organo-bridged dicobaloximes are reported.

2. Results and discussion

2.1. X-ray diffraction structure analysis

μ-Polymethylene bridged dicobaloximes have been known for over 40 years, nevertheless, their crystal structures have not been reported due to the difficulty in growing qualified single crystals. After many attempts, red crystals of **1**, **2**, and **3** were obtained by slow evaporating the solution of them with CH_2Cl_2/CH_3CH_2OH(1:2) in the dark. Crystal data for dicobaloxime complexes **1**–**3** are listed in Table 1. The Diamond pictures with atomic numbering for them are depicted in Fig. 1. The selected bond lengths (Å) and angles (°) are listed in Tables 2 and 3, respectively.

Fig. 1 shows that in the three dicobalt complexes two similar cobaloxime units are bridged by a polymethylene chain. Each cobaloxime has octahedral configuration with four nitrogen atoms of the dmgH units at equatorial, one carbon atom of the polymethylene group and one nitrogen atom of the pyridine group at axial positions. Four nitrogen atoms from the each dmgH unit in dicobaloxime complex are obviously coplanar. All the bond lengths and angles involving the two cobalt atoms are comparable to those reported for monocobaloximes [9–11]. It is noted that

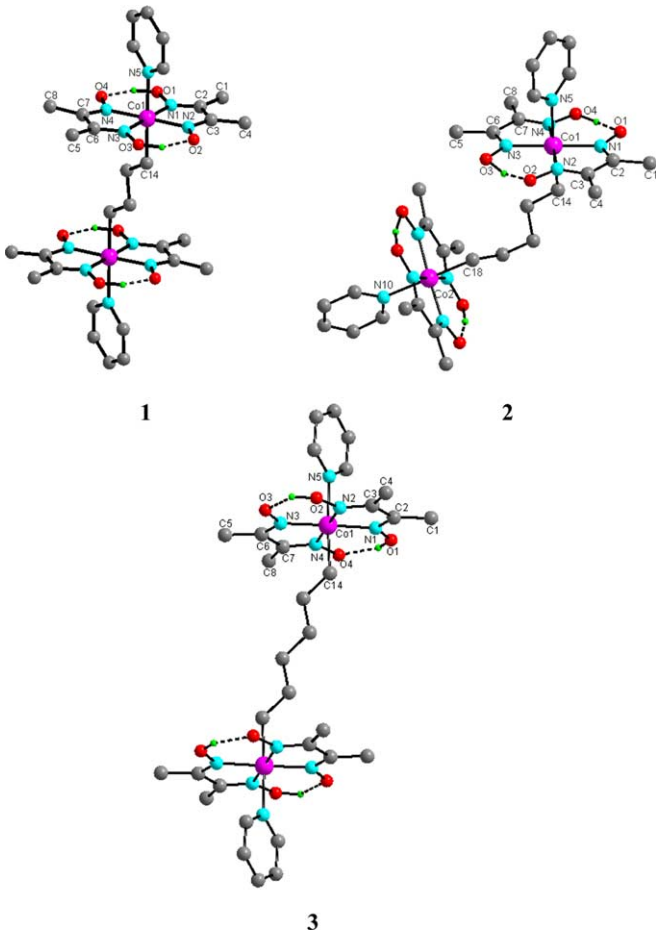

Fig. 1. Structures and numberings of complexes **1**–**3** (for clarity, most of the hydrogen atoms are omitted). The crystallized solvent molecules are not included.

the angle between the two $Co(dmgH)_2$ units is 64.1° and two parts of $Co(dmgH)_2$ are un-equivalent in **2**. While in the cases of **1** and **3**, those angles are almost 0°, and the building blocks are formed by a symmetric operation on

Table 1
Crystal data for complexes **1**–**3**

	1 · $2CH_2Cl_2$	**2**	**3** · CH_2Cl_2
Formula	$C_{30}H_{46}Co_2N_{10}O_8 \cdot 2(CH_2Cl_2)$	$C_{31}H_{48}Co_2N_{10}O_8$	$C_{32}H_{50}Co_2N_{10}O_8 \cdot CH_2Cl_2$
fw	962.48	806.65	905.61
Crystal size (mm)	$0.32 \times 0.24 \times 0.22$	$0.30 \times 0.25 \times 0.20$	$0.20 \times 0.20 \times 0.10$
Temperature (K)	293	293	293
Crystal system	Monoclinic	Triclinic	Triclinic
Space group	$P2_1/n$	$P\bar{1}$	$P\bar{1}$
a (Å)	8.9310(18)	8.4460(10)	8.2620(17)
b (Å)	18.151(4)	14.189(2)	8.8350(18)
c (Å)	13.635(3)	15.764(2)	16.067(3)
V (Å^3)	2188.9(8)	1830.4(4)	1040.8(5)
α (°)	90	83.460(2)	89.13(3)
β (°)	97.98(3)	88.330(3)	84.94(3)
γ (°)	90	77.230(2)	63.03(3)
Z	2	2	1
R	0.0605	0.0561	0.0589
wR_2	0.1287	0.1237	0.1125

Table 2
Selected structural parameters for **1**–**3**

	1 · $2CH_2Cl_2$	**3** · CH_2Cl_2	**2a**[a]		**2b**[a]
Co1–N5 (Å)	2.049(3)	2.066(4)	2.061(3)	Co2–N10 (Å)	2.092(4)
Co1–C14 (Å)	1.998(3)	2.036(5)	2.003(4)	Co2–C18 (Å)	2.022(5)
C_α–C_β	1.526(4)	1.447(6)	1.494(6)	C_α–C_β	1.528(7)
N5–Co1–C14 (°)	179.66(14)	176.67(19)	176.41(16)	N10–Co2–C18 (°)	177.68(16)
Co1–C_α–C_β (°)	119.3(2)	123.6(4)	118.6(3)	Co2–C_α–C_β (°)	118.9(3)
$N_1N_2N_3N_4$[b] (Å)	0.0067	0.0092	0.0153	$N_6N_7N_8N_9$[b] (Å)	0.0053
α[c] (°)	2.5	1.5	1.6	α[c] (°)	1.3
d[d] (Å)	0.0108	0.0255	0.0293	d[d] (Å)	0.0456
Co···Co(Å)	7.423	10.032	7.680		

[a] There are two un-equivalent $Co(dmg)_2$ units in complex **2**. **2a** is assigned to Co(1), **2b** is assigned to Co(2).
[b] Mean deviation from the equatorial plane of four donor atoms $N_1N_2N_3N_4$ or $N_6N_7N_8N_9$.
[c] Butterfly-bending angle between the two oxime planes.
[d] Displacements of Co atom from the $N_1N_2N_3N_4$ plane or $N_6N_7N_8N_9$.

Table 3
C–H···O hydrogen bonds in **1** · $2CH_2Cl_2$, **2** and **3** · CH_2Cl_2

Bond	Distance (Å)			Angle (°)
	C–H	H···O	C···O	C–H···O
1 · $2CH_2Cl_2$				
C1–H1B···O4	0.9600	2.5900	3.532(6)	165.00
C16–H16A···O1	0.9700	2.4900	3.207(8)	131.00
C10–H10···O4	0.9300	2.6140	3.207(8)	137.28
2				
C10–H10A···O6	0.9300	2.3000	3.033(6)	135.00
C29–H29A···O6	0.9298	2.6968	3.470(6)	141.06
C11–H11A···O8	0.9305	2.6432	3.183(5)	117.58
C30–H30A···O3	0.9294	2.6348	3.409(6)	141.15
3 · CH_2Cl_2				
C10–H10···O1	0.9300	2.4200	3.260(5)	150.00
C15–H15A···O3	0.9702	2.6153	3.537(6)	158.81
C12–H12···O1	0.9304	2.7120	3.350(6)	126.49

one asymmetric unit and thus both of them are centrosymmetric. Complexes **1** and **3** crystallize with dichloromethane solvent molecules, respectively, and in **3** the methylene chloride is disordered with half occupancy. In addition, there are some special structural features among the three complexes, which are summarized in the following:

2.1.1. Deformation of the $Co(dmgH)_2$ units

Generally, due to its flexibility [25], the $Co(dmgH)_2$ unit in organo-cobaloxime complexes may undergo geometrical deformations, whose extent could be represented by the displacement of the cobalt out of the equatorial 4-nitrogen plane (d) and by the butterfly-bending angle between the two dmgH units (α) [9–11]. The same structural features are found in our μ-polymethylene bridged dicobaloximes. From Table 2, we can see that in **1**, **2**, and **3** the α values are all very small and positive, which means that $Co(dmgH)_2$ units in our dicobaloxime complexes are almost flat. While the displacement, d, increases in the order **1** < **3** < **2a** < **2b** (0.0108, 0.0255, 0.0293, and 0.0456 Å, respectively).

2.1.2. Bond distances around cobalt

Usually, the Co–C bond and Co–L bond distances in alkylcobaloxime complexes are influenced by the steric hindrance or electronic effects from both the axial alkyl and base group [9–11]. For our dicobaloximes, the Co–C distances of **1**–**3** are all in the common range of Co–C bond, i.e., 1.99–2.09 Å [9–11]. In complex **1**, the Co–C bond distance of 1.998(3) Å is very close to that found for $CH_3Co(dmgH)_2py$ (1.998(5) Å) [26], but shorter than those reported for $CH_3CH_2Co(dmgH)_2py$ (2.061(15) Å) [27] and *i*-$C_3H_7Co(dmgH)_2py$ (2.085(3) Å) [28]. In comparison to the obvious increase of Co–C bond distance with the increasing bulk of the alky group in monocobaloxime complex, the Co–C bond distance lengthens very slightly from 1.998(3) Å in **1** to 2.036(5) Å in **3**. Basically, the Co–N bond distances of dicobaloxime complexes (2.049(3), 2.061(3) and 2.066(4) Å in **1**–**3**, respectively), are close to that reported for CH_3Co-$(dmgH)_2py$ (2.068(3) Å), except one longer bond distance in **2** (2.092(4) Å). In general, it seems that the Co–C and Co–N bond lengths do not significantly influenced by the chain length of the alkyl bridge, and the small changes in bond distances probably can be attributed to crystal packing effect.

It is of quite interest to compare the structural parameters of **1**–**3** with that of vitamin B_{12} dimer tetramethylene-1,4-di-Coβ-cobalamin (**D4**) [17], where the mean corrin rings of the two cobalamin units of **D4** are almost parallel (tilt of 2.3°). Practically, the Co–C distance of **1** (1.998(3) Å) and **2a** (2.003(4) Å) is almost identical to that of **D4** (2.001 Å), and those of **2b** (2.022(5) Å) and **3** (2.036(5) Å) are a little longer than that in **D4**. It is note worthy that the Co–N distance of **D4** (2.202 Å) is significantly longer than those in **1**–**3**. It clearly appears that the steric interaction between the bulkier dimethylbenzimidazole of **D4** and the more crowed corrin unit, as compared with that in cobaloxime, should be responsible for such big increase.

In addition, there are two un-equivalent $Co(dmgH)_2$ units in **2**. All the geometric parameters for **2a** and **2b**

units are different (see Table 2). Probably, it reflects the various environments of the two ends of the molecule, which will be discussed in the crystal packing section.

2.1.3. Conformation of bridged alkyl chain

It is interest to note that in comparison of the Co···Co distance for the same alkylene bridged dicobalt complexes, unequal separations of Co···Co are found for **1** (7.423 Å) and **D4** (6.948 Å), respectively. The reason for that is probably due to different conformations adopted by the tetramethylene bridges in them (Fig. 2). In B_{12} dimer **D4**, the tetramethylene bridge presents with a strained *gauche*-conformation as a result of its constitution and of intra-molecular packing effects [17]. While in case of **1**, it appears to be in a unstrained *anti*-conformation. Similarly, the hexamethylene chain that bridges the two cobalt centers of **3** at a distance of 10.032 Å is also in a predominately "relaxed" *anti*-conformation. Whilst, in **2**, where there is an angle of 64.1° between the two $Co(dmgH)_2$ units, the Co···Co separation is only 7.680 Å, very close to that of **1**. This is probably due to the pentamethylene bridge presents a strained *gauche*-conformation causing tight arrangement of the two $Co(dmgH)_2$ units. By using ^{13}C NMR technique, Hannak and co-workers [16] have reported that in aqueous solutions the dodecamethylene bridge adopt *gauche*-conformation in organometallic B_{12} dimer and *anti*-conformation in organometallic B_{12} rotaxane.

2.2. Packing structure

Recently, inter and intra-molecular weak interactions of monocobaloximes have been discussed by Gupta et al. [29,30]. In our cases, it is of interest to note that prismatic crystal **2** can be stored in air for months, however, claviform crystals **1** and **3** would effloresce within a few minutes once exposure to air. In order to elucidate the different stabilities for the title solid-state complexes, their packing structures are worth investigating. Structures **1**, **2** and **3** propagate as 2-D layers through C–H···O intermolecular hydrogen bonds involving one or two hydrogen atoms from pyridine and one dioxime oxygen (Table 3 and Fig. 3). In **3** there is another C–H···O intermolecular hydrogen bond, at which the hydrogen atoms from alkyl chain act as donors and the dioxime oxygen atoms act as acceptors. Further, the 2-D layer structures build up 3-D structures via other C–H···O interactions in **2** and **3**, respectively.

Besides, in structure **1** crystallized CH_2Cl_2 molecules, which fill in a larger channel (9.82×7.50 Å^2) surrounded by dicobaloximes, also participate in the H-bonded networks. While in **3**, CH_2Cl_2 molecules stay in a narrow channel (5.82×4.25 Å^2), resulting in the comparably tight fit of the solvent molecules.

2.3. Kinetic studies

Photolytic kinetic properties of μ-polymethylene bridged dicobaloximes were investigated and the observed rate of Co–C bond cleavage were measured by UV–Vis spectroscopy. The λ_{max} of dicobaloximes of the Co–C CT band of the four complexes are around 450 nm, which are similar to those observed in monocobaloximes [9].

As an example, the absorbance change of UV–Vis in photolysis and the plot of the observed rate constant for **2** in methanol are shown at Fig. 4. It can be seen that during photolysis absorbance at 450.5 nm gradually decreases and that the shoulder at 380 nm increases. There has been observed two isobestic points at 423 and 500 nm, respectively. Similar spectra changes have been observed in **1**, **3** and **4**.

The decomposition process of Co–C bond of all the dicobaloximes obeys a pseudo-first-order rate law. Through UV–Vis study, we determined the observed photolytic rate constants of **1**–**4** and summarized in Table 4. As we can see there is no much difference in the observed photolytic rate constants with changing the alkyl length in methanol. Furthermore, it has been observed that the rate

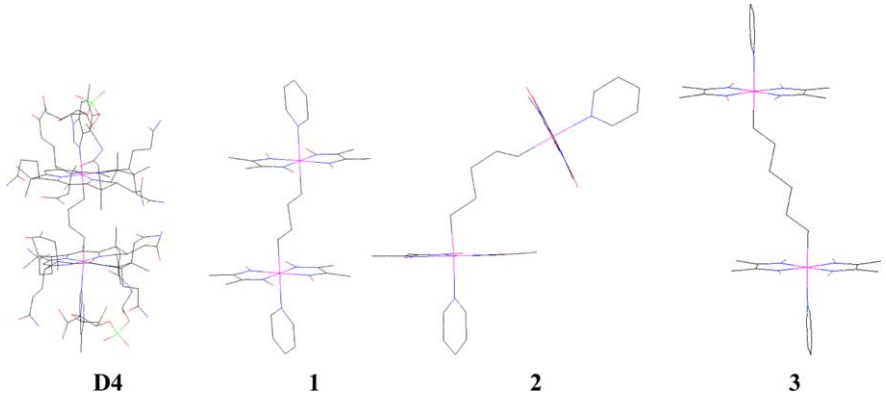

Fig. 2. Conformation of bridged alkyl chain of **D4** and **1**–**3**.

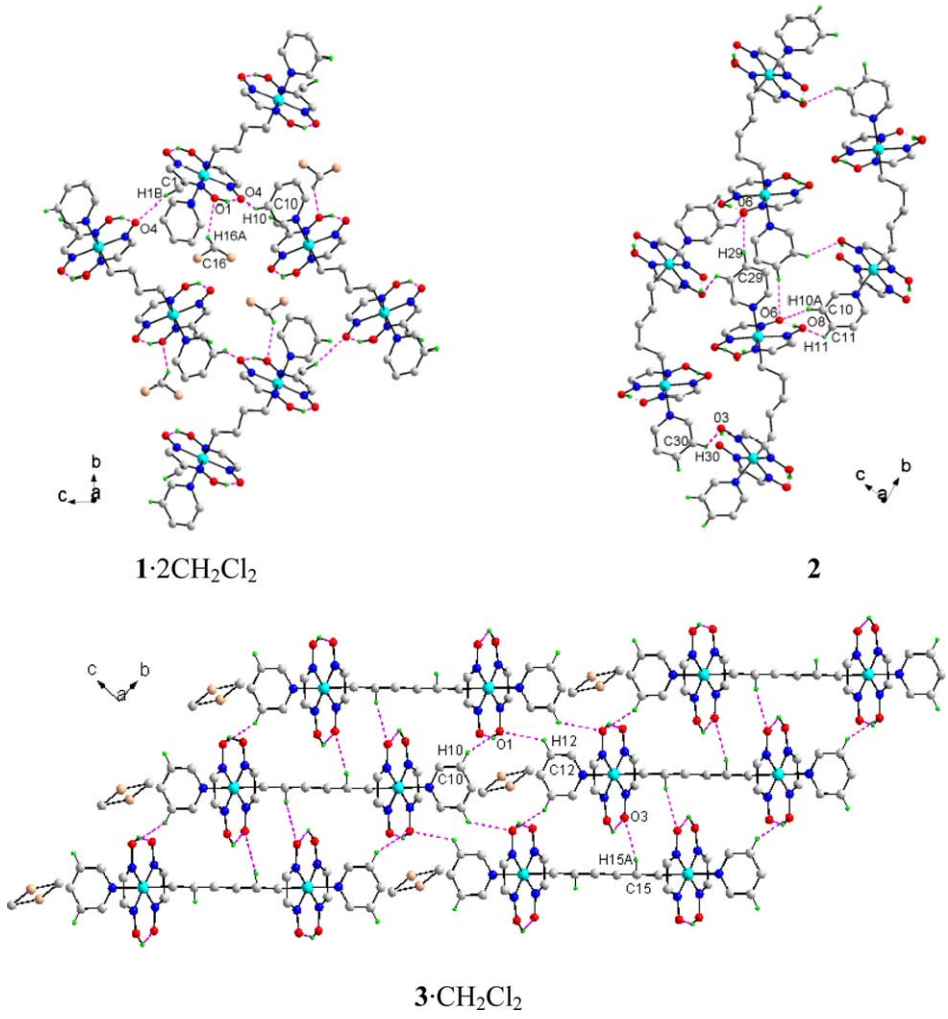

Fig. 3. The layered structures of **1**–**3** through C–H···O interactions (for clarity methyl carbon atoms in dmgH and all other hydrogen atoms are not shown).

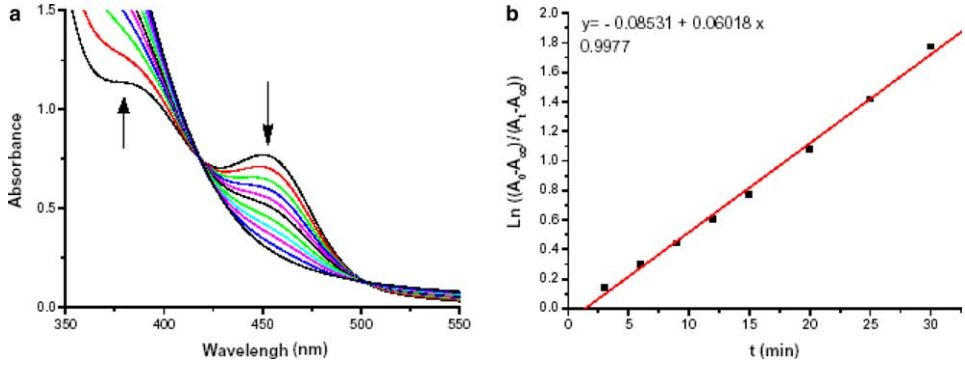

Fig. 4. UV–Vis change at 25 °C (a) and the observed rate constant (b) of **2** in methanol.

constants systematically increase in changing the solvent from methanol to ethanol. Probably, the solvent molecules are involved in the transition state during the photolysis process [31,32]. In addition, there is no big enhancement of the observed rates constants between monocobaloxime $pyCo(dmgH)_2(CH_2)_4CH_3$ ($1.21 \times 10^{-3}\ s^{-1}$) and dicobaloxime **2** ($1.02 \times 10^{-3}\ s^{-1}$) in methanol, which have same methylene length. Therefore, it is suggested that in solution one cobaloxime unit has no effect on the other unit.

2.4. ESI-MS investigation of the products from photolysis

The photolytic methanol solution of complex **1** was examined by ESI-MS. There are seven intense peaks in

Table 4
The observed photolytic rate constants for **1**–**4**

	Observed rate constant (s^{-1})	
	In methanol	In ethanol
1	$8.42(5)\times10^{-4}$	$1.16(5)\times10^{-3}$
2	$10.20(2)\times10^{-4}$	$1.38(5)\times10^{-3}$
3	$9.92(3)\times10^{-4}$	$1.33(3)\times10^{-3}$
4	$8.50(5)\times10^{-4}$	$1.19(4)\times10^{-3}$

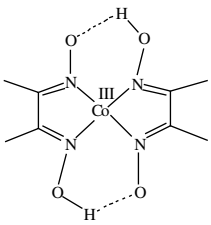

6. (M_6=289)

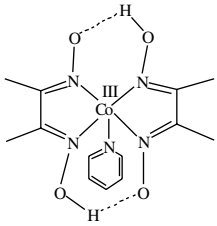

7. (M_7=368)

its spectrum after 1.5 h of photolysis (see Fig. 5), and their assignments are shown in Table 5. The peak at *m/z* 289.1 may be assigned to de-pyridine bis(dimethylglyoxime)-cobalt(III) $[M_6]^+$, and the peak at *m/z* 367.9 corresponds to pyridine bis(dimethylglyoxime)cobalt(III) $[M_7]^+$, respectively. The most intense signal at *m/z* 798.9 can be assigned to $2[M_7 + CH_3OH]^+$, i.e., adduct of two methanols and dimeric of species 7.

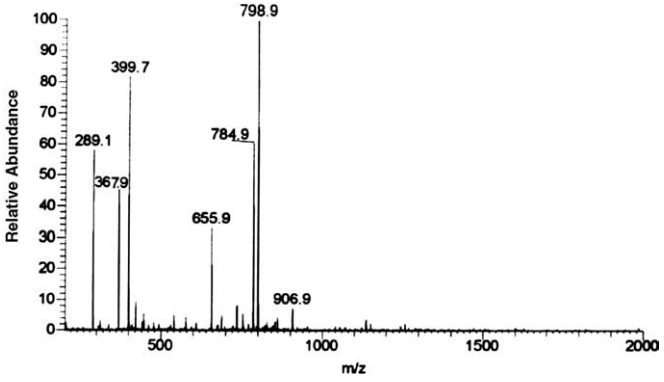

Fig. 5. ESI-MS spectrum for photolytic products of **1**.

Table 5
The assignment for peaks of **1**

Mass charge ratio (*m/z*)	Relative abundance	Assigned species
289.1	58	$[M_6]^+$
367.9	45	$[M_7]^+$
399.7	82	$[M_7+CH_3OH]^+$
655.9	32	$[M_6 + M_7]^+$
784.9	60	$[M_6 + M_7 + 4CH_3OH]^+$
798.9	100	$2[M_7 + CH_3OH]^+$
906.9	7	$2[M_7 + CH_3OH + 3H_2O]^+$

The peaks at *m/z* 399.7, 655, 785 and 906.9 are assigned to adduct of two or more species, respectively (see the details at Table 5). The photolytic products characterized by ESI-MS are cobalt(III) species, which is the oxidized Co(II) species produced from the Co–C bond breaking. Similar ESI-MS active species have been generated from the photolysis of **2**, **3** and **4**, with relative abundance slightly different. However, the photolysis products of **1**–**4** in ethanol are different from those in methanol and we cannot explain them clearly now. Organic species could not be characterized by ESI-MS because they are in gas phase in normal temperature.

2.5. Thermogravimetric analysis

TGA and DTA data of **1**–**4** are summarized in Table 6. TGA and DTA scans for **3** and **4** are shown at Figs. 6 and 7, respectively. TGA and DTA scans for **1** and **2** are supplied as supplementary material.

It is noted that there is no weight-loss at 10–150 °C for **1**, while 3% weight-loss around 100 °C for **3** (Fig. 6). The results indicate that the CH_2Cl_2 solvent molecules for **1** and **3** are in various circumstances. As mentioned before, CH_2Cl_2 molecules of **1** in a larger hole thus they are easier to escape at room temperature, and those of **3** in a smaller hole (see the packing structures at Fig. 3) are lost during heating. In the range of 150–500 °C, the thermal decomposition of the dicobaloximes **1**–**4** includes two transitions. The first transition of **1**–**4** (150–280 °C) corresponds to a loss of two axial pyridine ligands, a polymethylene and four HNO_2 molecules [33,34]. This process is mainly the cleavage of axial ligands, but accompanying the decomposition of part equatorial ligand. The elimination of HNO_2 at this stage is confirmed by the test with sulfanilicacid and α-naphthylamine [33]. The second transition (280–500 °C) involves the decomposition of the common 'core'

Table 6
TGA and DTA data for **1**–**4**

	Weight-loss exp. (calc.)	Loss substance	Temperature range of weight-loss (°C)	T_1 (°C)[a]	T_2 (°C)[a]
1	46.3(50.7)	2py, $(CH_2)_4$, $4HNO_2$	150–264	236	273
2	47.1(51.5)	2py, $(CH_2)_5$, $4HNO_2$	150–266	221	277
3	46.5(50.3)	2py, $(CH_2)_6$, $4HNO_2$	150–267	228	279
4	62.8(56.7)	2py, $(CH_2)_{12}$, $4HNO_2$	150–280	197, 260	331

[a] T_1 and T_2 are taken as the peak temperatures in the DTA.

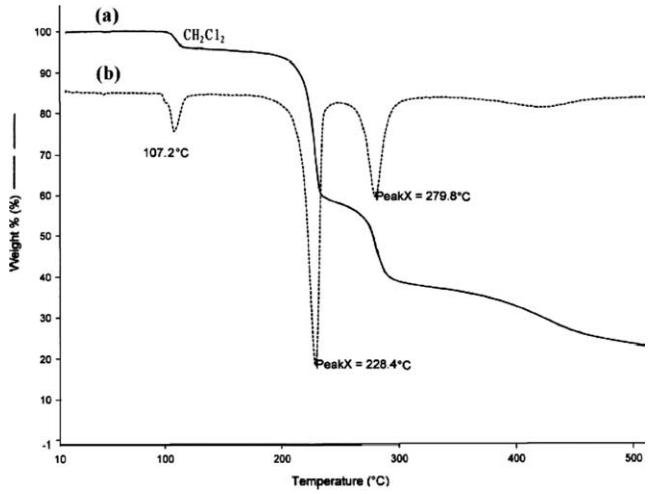

Fig. 6. (a) Thermogravimetric analysis (TGA) and (b) first derivative curves of TG scans of **3**.

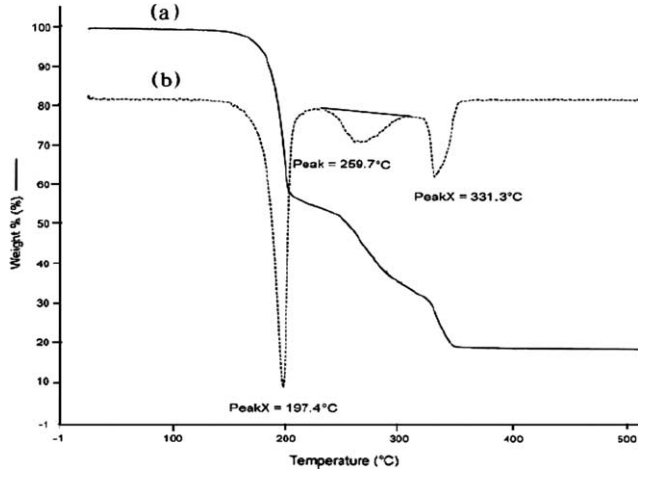

Fig. 7. (a) Thermogravimetric analysis (TGA) and (b) first derivative curves of TG scans of **4**.

complexes (bis(dimethylglyoximato)cobalt(II)) [33,34]. In addition, the DTA diagram of **4** shows different characteristics (Fig. 7). There has been observed two DTA peak temperatures (197 and 260 °C) during the process of loss of two axial pyridine molecules and an polymethylene chain $-(CH)_{12}-$.

3. Conclusions

In the present work, crystal structures of a series of μ-polymethylene bridged dicobaloximes (**1**–**3**) are reported. Their interesting structural features such as distances around cobalt, deformation of $Co(dmgH)_2$ unit, conformation of bridged alkyl chain, and crystal packing are discussed and compared. In addition, similar thermal decomposition process and photolytic rates are observed for the μ-polymethylene bridged dicobaloximes (**1**–**4**).

4. Experiment

4.1. Synthesis

μ-Polymethylene bridged dicobaloximes were prepared according to the methods of literature [21]. The purification procedure of these complexes was modified in this work by crystallization from the CH_2Cl_2/CH_3CH_2OH (1:2) solution instead of silica gel column separation. The crystals were dried in vacuum before element analysis.

$py(dmgH)_2Co(CH_2)_4Co(dmgH)_2py \cdot 2CH_2Cl_2$ (**1** · $2CH_2Cl_2$) Anal. Calc. for $C_{30}H_{46}Co_2N_{10}O_8$: C, 45.46; H, 5.85; N, 17.67. Found: C, 45.40; H, 5.80; N, 17.61%. Crystallized CH_2Cl_2 molecules were completely lost after drying. ^1H NMR (Bruker, 500 MHz, $CDCl_3$): py 8.59 (d, 4H), 7.71 (t, 2H), 7.31 (t, 4H); CH_3 2.14(s, 24H); Co–CH_2 1.58(t, 4H); Co–CH_2–CH_2 0.88 (bm, 4H). ESI-MS (LCQ-Finnigan): $m/e = 792.6(M + H)^+$.

$py(dmgH)_2Co(CH_2)_5Co(dmgH)_2py$ (**2**) Anal. Calc. for $C_{31}H_{48}Co_2N_{10}O_8$: C, 46.16; H, 6.05; N, 17.36. Found: C, 46.22; H, 6.12; N, 17.47%. ^1H NMR (Bruker, 500 MHz, $CDCl_3$): py 8.57 (d, 4H), 7.72 (t, 2H), 7.33 (t, 4H); CH_3 2.12 (s, 24H); Co–CH_2 1.56 (t, 4H); Co–CH_2–CH_2 0.86 (bm, 4H); Co–CH_2–CH_2–CH_2 1.06 (bm, 2H). ESI-MS (LCQ-Finnigan): $m/e = 806.6(M + H)^+$.

$py(dmgH)_2Co(CH_2)_6Co(dmgH)_2py \cdot CH_2Cl_2$ (**3** · CH_2Cl_2) Anal. Calc. for: $C_{32}H_{50}Co_2N_{10}O_8 \cdot 0.3CH_2Cl_2$: C, 45.85; H, 6.03; N, 16.55. Found: C, 45.92; H, 6.03; N, 16.66%. Crystallized CH_2Cl_2 molecules were partly lost after drying. ^1H NMR (Bruker, 500 MHz, $CDCl_3$): py 8.60(d, 4H), 7.71(t, 2H), 7.30(t, 4H); CH_3 2.12 (s, 24H); Co–CH_2 1.60(t, 4H); Co–CH_2–CH_2 0.83 (bm, 4H); Co–CH_2–CH_2–CH_2 1.12 (bm, 4H). ESI-MS (LCQ-Finnigan): $m/e = 820.7(M + H)^+$.

$py(dmgH)_2Co(CH_2)_{12}Co(dmgH)_2py$ (**4**) Anal. Calc. for $C_{38}H_{62}Co_2N_{10}O_8$: C, 50.44; H, 6.91; N, 15.48. Found: C, 50.24; H, 7.01; N, 15.55%. ^1H NMR (Bruker, 500 MHz, CDCl3): py 8.59 (d, 4H), 7.70 (t, 2H), 7.30 (t, 4H); CH_3 2.12 (s, 24H); Co–CH_2 1.60 (t, 4H); Co–CH_2–CH_2 0.87 (bm, 4H); Co–CH_2–CH_2–CH_2 1.23 (bm, 16H). ESI-MS (LCQ-Finnigan): $m/e = 905.6(M + H)^+$.

$pyCo(dmgH)_2(CH_2)_4CH_3$ (**5**) Anal. Calc. for $C_{18}H_{30}CoN_5O_4$: C, 49.20; H, 6.88; N, 15.94. Found: C, 48.90; H, 6.92; N, 15.84%. ^1H NMR (Bruker, 500 MHz, $CDCl_3$): py 8.59 (d, 2H), 7.65 (t, 1H), 7.24 (t, 2H); CH_3 2.10 (s, 12H); Co–CH_2 1.64 (t, 2H); Rest alkyl chain: 0.80–1.37. ESI-MS (LCQ-Finnigan): $m/e = 439.4(M + H)^+$.

4.2. Photolytic kinetic studies

All samples for photolysis were prepared in methanol solutions at 25 °C under the anaerobic condition and in the red light. The solution with concentration about 5×10^{-4} M was loaded into a quartz cuvette (1 cm

path-length) and degassed for 30 min by nitrogen gas through it. Lastly, the cuvette for anaerobic sample was sealed with a Teflon cap under positive nitrogen pressure, and exposed to a 8 W white light lamp, which was placed at a distance of 10 cm. The absorbance changes of the UV–Vis spectra during photolysis were recorded by UV/3100.

The photolytic kinetic measurements were performed under pseudo-first-order conditions and the reactions followed at least 3 half-lives. A_0 and A_∞ are taken from the experiment value. The observed rate constants were calculated by linear least-squares regression using the formula:

$$\ln\frac{A_0 - A_\infty}{A_t - A_\infty} = kt.$$

The ESI-MS measurements of photolysis products of all complexes were carried out on a LCQ-Finnigan at room temperature. The mobile phase is methanol/water (1:1).

4.3. Thermogravimetric analysis

TGA experiments were performed on a Perkin–Elmer 7 Series Thermal Analysis system. The flow rate of nitrogen was about 20 ml/min. A heating rate of 10 °C/min was employed. Samples (1–4 mg) were dried over P_2O_5 in vacuum before used.

5. Crystal structure determination

Raw intensities for **1** and **3** were collected using a Siemens P4 four-circle diffractometer with monochromated Mo Kα ($\lambda = 0.71073$ Å) radiation. Raw intensities for **2** were collected using a Bruker's SMART CCD area detector diffractometer operating in the $\omega - 2\theta$ scan mode with graphite-monochromated Mo Kα radiation ($\lambda = 0.71073$ Å). The three structures were solved by directed methods using the program SHELXTL [35]. All the non-hydrogen atoms were located from the trial structure and then refined anisotropically with SHELXTL using full-matrix least-squares procedures. The two bridging oxime protons were found in difference Fourier map. The final difference Fourier map was found to be featureless. Crystallographic data for the structural analysis of **1**–**3** have been deposited with the Cambridge Crystallographic Data Center, CCDC Nos. 256773–256775. Copies of this information can be obtained free of charge from The Director, 12, Union Road, Cambridge CB2 1EZ, UK (fax: +44 1223 336033; e-mail: deposit@ccdc.cam.ac.uk or http://www.ccdc.cam.ac.uk).

Acknowledgements

This work was supported by the National Natural Science Foundation of China (No. 20071017, 50272029) and the Research Found for the Doctoral Program of Higher Education (No. 2000028401).

Appendix A. Supplementary data

Supplementary data associated with this article can be found, in the online version, at doi:10.1016/j.jorganchem.2005.10.015.

References

[1] B.P. Branchaud, M.S. Meier, M.N. Malekzadeh, J. Org. Chem. 52 (1987) 212.
[2] J. Halpern, Science 227 (1985) 869.
[3] R. Banerjee, Chemistry and Biochemistry of B_{12}, Wiley, New York, 2000.
[4] J. Halpern, S.H. Kim, T.W. Leung, J. Am. Chem. Soc. 106 (1984) 8317.
[5] R.G. Finke, B.P. Hay, Inorg. Chem. 23 (1984) 3041.
[6] H.L. Chen, H. Yan, L.B. Luo, X.X. Cui, W.X. Tang, J. Inorg. Biochem. 66 (1997) 219.
[7] A.G. Cole, L.M. Yoder, Y.J. Shiang, N.A. Anderson, L.A. Walker, R.J. Sension, J. Am. Chem. Soc. 124 (2002) 434.
[8] C. Michael-Elliott, E. Hershenhart, R.G. Finke, B.L. Smith, J. Am. Chem. Soc. 103 (1981) 5558.
[9] N. Bresciani-Pahor, M. Forcolin, L.G. Marzilli, L. Randaccio, M.F. Summers, P.J. Toscano, Coord. Chem. Rev. 63 (1985) 1.
[10] L. Randaccio, N. Bresciani-Pahor, E. Zangrando, L.G. Marzilli, Chem. Soc. Rev. 18 (1989) 225.
[11] L. Randaccio, Comments Inorg. Chem. 21 (1999) 327.
[12] E.L. Smith, L. Mervyn, P.W. Muggleton, A.W. Johnson, N. Shaw, Ann. NY Acad. Sci. 112 (1964) 565.
[13] G.N. Schrauzer, R.J. Windgassen, J. Am. Chem. Soc. 88 (1966) 3738.
[14] S.N. Anderson, D.H. Ballard, M.D. Johnson, J. Chem. Soc., Perkin Trans. 2 (1972) 311.
[15] K.P. Finch, J.R. Moss, J. Organomet. Chem. 346 (1988) 253.
[16] R.B. Hannak, G. Färber, R. Konrat, B. Kräutler, J. Am. Chem. Soc. 119 (1997) 2313.
[17] B. Kräutler, T. Dérer, P. Liu, W. Mühlecker, M. Puchberger, K. Gruber, C. Kratky, Angew. Chem. Int. Ed. Engl. 34 (1995) 84.
[18] B.D. Gupta, K. Qanungo, J. Organomet. Chem. 534 (1997) 213.
[19] H. Shimakoshi, A. Goto, Y. Tachi, Y. Naruta, Y. Hisaeda, Tetrahedron Lett. 42 (2001) 1949.
[20] H. Shimakoshi, M. Koga, Y. Hisaeda, Bull. Chem. Soc. Jpn. 75 (2002) 1553.
[21] B.D. Gupta, V. Vijaikanth, V. Singh, Organometallics 23 (2004) 2069.
[22] J.R. Moss, J. Organomet. Chem. 231 (1982) 229.
[23] J.R. Moss, L.G. Scott, Coord. Chem. Rev. 60 (1984) 171.
[24] C.P. Casey, J.D. Audett, Chem. Rev. 86 (1986) 339.
[25] M.K. Geno, J. Halpern, J. Am. Chem. Soc. 109 (1987) 1238.
[26] A. Bigotto, E. Zangrando, L. Randaccio, J. Chem. Soc., Dalton Trans. (1976) 96.
[27] Yu.A. Simonov, A.I. Shkurpelo, N.M. Samus, E.L. Belokoneva, I.D. Samus, Koord. Khim. 6 (1980) 1107.
[28] L.G. Marzilli, P.J. Toscano, L. Randaccio, N. Bresciani-Pahor, M. Calligaris, J. Am. Chem. Soc. 101 (1979) 6744.
[29] B.D. Gupta, Veena Singh, R. Yamuna, T. Barclay, W. Cordes, Organometallics 22 (2003) 2670.
[30] D. Mandal, B.D. Gupta, Organometallics 24 (2005) 1501.
[31] N.E. Brash, A.G. Cregan, M.E. Vanselow, J. Chem. Soc., Dolton Trans. (2002) 1287–1294.
[32] C. Eaborn, I.D. Jenkins, G. Seconi, J. Organomet. Chem. 131 (1977) 387.
[33] A.V. Benedetti, M. Ionashiro, Thermochim. Acta. 91 (1985) 391.
[34] K.L. Brown, G.W. Jang, R. Segal, K. Rajeshwar, Inorg. Chim. Acta. 128 (1987) 197.
[35] G.M. Sheldrick, SHELXTL, Version 5.1, Bruker AXS, Inc., Madison, WI, 1997.